Bull. Chem. Soc. Ethiop. **2026**, 40(10), 2205-2220.
DOI: https://dx.doi.org/10.4314/bcse.v40i10.11

ISSN 1011-3924
Printed in Ethiopia
Online ISSN 1726-801X

SYNTHESIS, DFT INVESTIGATION, AND BIOLOGICAL EVALUATION OF A NOVEL Au(III) SCHIFF BASE COMPLEX WITH ANTIOXIDANT AND ANTICANCER ACTIVITIES

Marwan Hadi Hussein[1*], Haider Obaid Jamel[2], Sundus Kareem Hamzah[3]

[1]Ministry of Education, The General Directorate of Education in Qadisiyah, Qadisiyah, Iraq
[2]Al-Qadisiyah University / College of Education - Department of Chemistry
[3]Al-Qadisiyah University / College of Education - Department of Chemistry

(Received October 30, 2025; Revised July 1, 2026; Accepted July 6, 2026)

ABSTRACT. A novel Schiff base ligand, 2-((Z)-((3-((E)-((benzo[d]oxazol-2-yl) imino) methyl)pyridin-2-yl)imino)methyl)phenol (BOYMPIMP), and its Au(III) complex were synthesized and characterized. To the best of our knowledge, this is the first reported Au(III) complex derived from this ligand. The ligand was prepared by Schiff base condensation, and the complex was synthesized using a 1:1 metal-to-ligand molar ratio. Structural characterization was performed using FTIR, UV–Vis, ^{1}H and ^{13}C NMR, CHN analysis, molar conductivity, and magnetic susceptibility, confirming a square-planar Au(III) coordination environment. DFT calculations at the B3LYP/6-311G(d,p) level supported the proposed structure and revealed a HOMO–LUMO energy gap of 7.662 eV, indicating high electronic stability. Antioxidant activity was evaluated by DPPH, ABTS, and FRAP assays. The Au(III) complex exhibited significantly higher antioxidant activity than the free ligand, comparable to ascorbic acid. Cytotoxicity was assessed against MCF-7 and MCF-10A cell lines using the MTT assay. The Au(III) complex showed greater activity toward MCF-7 cells (IC_{50} = 57.68 μg mL^{-1}) than the ligand (IC_{50} = 173.4 μg mL^{-1}), with lower toxicity toward MCF-10A cells (IC_{50} = 279.3 μg mL^{-1}), indicating selective anticancer potential. These findings identify the Au(III) complex as a promising antioxidant and anticancer candidate for further investigation.

KEY WORDS: Schiff bases, Au(III) complex, DFT, Antioxidant, Anticancer, Benzoxazole

INTRODUCTION

Since global cancer burden estimates were first published in the 1980s, breast cancer has been the cancer most diagnosed among females [1, 2]. Today, it remains the leading cancer diagnosis and cause of cancer-related death in females, and is a major contributor to the cancer burden even when both sexes are combined, representing the second most frequently diagnosed cancer and the fourth most common cause of cancer-related mortality in 2022 [3]. While breast cancer is a major cancer worldwide, it has long been recognized that the burden is not evenly distributed [4, 5]. Indeed, regional and country-specific differences in the underlying age structure, prevalence of risk factors, and healthcare infrastructure give rise to global patterns that determine how common and fatal breast cancer is in a given setting. In addition to their promising anti-proliferative activities against breast cancer cell lines [6], benzoxazole derivatives have also demonstrated significant potential in enhancing the efficacy of existing treatments by targeting specific metabolic pathways. For instance, recent studies have shown that these compounds can inhibit wild and mutated forms of the epidermal growth factor receptor (EGFR), which plays a critical role in cancer cell proliferation and survival [7]. Furthermore, the integration of molecular docking studies has revealed that these derivatives exhibit binding affinities comparable to current FDA-approved drugs, suggesting their viability as alternative therapeutic agents [8]. As researchers continue to explore the pharmacological landscape of benzoxazole derivatives, the synthesis of hybrid compounds that combine their properties with other pharmacophores could

*Corresponding authors. E-mail: adiraq69@gmail.com

pave the way for more effective and personalized breast cancer therapies [9]. Therefore, the present study aims to design, synthesize, and characterize novel metal complexes and evaluate their biological potential using experimental and computational approaches. Similar to most Au(III) complexes, Au(III) complexes can inhibit the activities of thiol-containing enzymes, including thioredoxin reductase, via ligand exchange reactions to form Au–S(Se) bonds.

Nonetheless, there are examples of physiologically stable Au(III) and Au(I) complexes,such as [Au(TPP)]Cl (H2TPP = 5,10,15,20-tetraphenylporphyrin) and [Au(dppe)2]Cl (dppe = 1,2-bis(diphenylphosphanyl)ethane), which are known to display highly potent in vitro and in vivo anticancer activities. In this study, In the present work of anticancer gold(III) complexes[10], including their mechanisms of action and the approaches complexes, including their mechanisms of action and the approaches adopted to improve their anticancer efficiency. Some recent examples of gold anticancer chemotherapeutics are highlighted.

In most situations, the gold complexes exhibit anticancer activities by targeting thioredoxin reductase (TrxR) or other thiol-rich proteins and enzymes and trigger cell death via reactive oxygen species (ROS). Interestingly, gold complexes were recently reported to elicit biochemical hallmarks of immunogenic cell death (ICD) as an ICD inducer.

In this study, the recent progress of gold(I) and gold(III) complexes is comprehensively summarized , and their activities and mechanism of action are documented. Therefore, the present work aims to design, synthesize, and characterize a novel benzoxazole-based Schiff base ligand and its corresponding Au(III) complex. The synthesized compounds were investigated using spectroscopic and analytical techniques, and their electronic properties were studied by Density Functional Theory (DFT) calculations. Furthermore, their antioxidant and in vitro anticancer activities against the MCF-7 breast cancer cell line were evaluated to explore their potential as promising bioactive Au(III)-based agents[11].

EXPERIMENTAL

Materials and apparatus

In this study, 2-aminobenzoxazole (98% purity, Merck), benzil (98%, Sigma-Aldrich), acetic acid (99%, BDH), and 2-aminonicotinic aldehyde (99%, Sigma-Aldrich) were used. At the same time,metal chlorides gold(III) were brought from Sigma-Aldrich. They were of varying purity: 99.9, 98, 97.5 and 99%, respectively. Also, the study used free radical 1,1-dipheny-l-2-picrylhydrazyl(DPPH), supplied by Sigma-Aldrich, for an antioxidant check. Breast cancer cell lines (MCF-7) and normal cell lines (MCF-10) were obtained from the Center for Natural Product Research and Drug Discovery, Department of Pharmacology, Faculty of Medicine, University of Baghdad. All chemicals used were of analytical grade and used without further purification.

2-aminobenzoxazole, benzyl acetic acid, and 2-aminonicotinaldehyde were obtained from commercial suppliers. Metal chlorides were used as received. Antioxidant activity was evaluated using the DPPH assay, while cytotoxicity was assessed using the MTT assay.

Synthesis of (BOYMPIMP) ligand and its complexes

Preparation of the ligand (BOYMPIMP): The ligand was prepared in two steps. was the preparation of (E)-3-((benzo[d]oxazol-2-ylimino)methyl)pyridin-2-amine (compound-B) from the reaction between 2-aminobenzoxazol (1.341 g, 0.002 mol) in 25 mL of absolute ethanol with 2-aminonicotinaldehyde (1.221 g, 0.002 mol) in 25 mL of absolute ethanol with continuous stirring. The mixture was refluxed for 8 h. After that, it was cooled, filtered, and collected. It was recrystallized by removing the residue of the starting material with 99.9% ethanol, allowing the precipitate to dry; then, it was collected and weighed to be employed in the second stage, yielding an 84% yield percentage. The 2-((Z)-((3-((E)-(benzo[d]oxazol-2-ylimino)methyl)pyridin-

2yl)imino)methyl)phenol (BOYMPIMP) was prepared by dissolving compound-B (0.400 g, 0.0015 mol) in 25 mL of ethanol with a solution of 2-hydroxybenzilaldehyde (0.194 g, 0.0053 mmol) in 25 mL of ethanol. Then, 5–6 drops of concentrated hydrochloric acid were added to the mixture with continuous stirring, and the mixture was refluxed for 8 h. It was cooled, precipitated, filtered, dried, and recrystallized using absolute ethanol. The product gave a yield of 79% and a melting point of 113 °C, as stated in Scheme 1.

Synthesis of the Au(III) complex

The complexes are prepared with a ratio of 1:1, which are as follows: Preparation of Au(III) complexes with BOYMPIMP ligand. The above complex was prepared using the same method, but at a different ratio, 1:1 M: L. BOYMPIMP ligand solution (0.3433 g, 0.002 mol) in 10 mL of ethanol was added to gold(III) chloride solution (0.393 g, 0.001 mol) in 10 mL of absolute ethanol. The mixture was refluxed for 2 h with stirring before being cooled, filtered, and dried.

Theoretical computational study

The ligand (BOYMPIMP) was studied using density functional theory (DFT) for all calculations, and the structure of the ligand (BOYMPIMP) was plotted using the GaussView program. The calculations were performed using Gaussian 09 with the DFT/P3LYP functional and the 6-311G core set, and the resulting structures were then processed with Multiwfn to analyze and calculate the theoretical electronic properties. As well as determining the total energy of the complex and the energy of the transition between the LUMO and the highest electron-occupied orbit, HOMO, and determining the energy difference between the orbits.

$$E_{gap} = E_{LUMO} - E_{HOMO} \quad (1)$$

$$\mu = \frac{E_{LUMO} + E_{HOMO}}{2} \quad (2)$$

$$x = -\mu \quad (3)$$

$$\eta = \frac{E_{LUMO} - E_{HOMO}}{2} \quad (4)$$

$$s = \frac{1}{2\eta} \quad (5)$$

$$\omega = \frac{\mu^2}{2\eta} \quad (6)$$

Measuring antioxidant capacity

The concentration of the tested compound, which causes 50% of radical scavenging activity (IC_{50}), was determined by the linear regression analysis from the obtained RSA values using GraphPad Prism 8.3.1 software. BOYMPIMP ligand and metal complexes were tested for radical scavenging activity against DPPH using a spectrophotometric method. In practice, 1 mL of the ligand and metal complexes in DMSO at various concentrations, 3.90-500 g/mL, was mixed with 1 mL of 0.1 mM DPPH in methanol. For 30 min, the tested samples were allowed to react with DPPH. After 30 min of incubation in the darkness at room temperature, the absorbance at 517 nm was measured with a Shimadzu UV-165PCS spectrophotometer. Then, the RSA% was calculated. The linear regression analysis was performed on the obtained RSA values to determine the IC_{50} value. The lower the value of IC_{50}, the more efficient the antioxidant [12] .

Biological activity (cytotoxic assay MTT)

In this study, two cell lines were used, namely the breast cancer cell line (MCF-7) and the normal human liver cell line (MCF-7). Cell lines were preserved in liquid nitrogen and were maintained and tested at the Biotechnology Research Center, University of Baghdad.

After the cells of cancer lines (MCF-7) and the suspension were completely prepared at a concentration of 1×105 cells/well, the cell suspension was placed in a plate containing 96 holes with a flat base, and it was incubated in an incubator with 5% carbon dioxide (CO_2) at a temperature of 37 °C, for 24 h. Then, 100 µL of this suspension was added to each well. After that, the concentrations that had been prepared for each of the ligands and the platinum complex, 25, 50, 100, 200, and 400 µg/mL, were added to those wells at the rate of three wells for each concentration. After that, the plate was incubated for a full day at an incubation temperature of 37°C, and 10 mL of MTT solution at a concentration of 0.45 mg/mL was added to each hole.

Then that plate was incubated for 4 h at 37 °C. 100 µL of DMSO solution was added to each hole and incubated for 5 min. Finally, the absorbance of that sample was read at a wavelength of 570 nm using the ELASIS device, and then the statistical analysis was conducted on the optical density readings to calculate the IC_{50} [13].

Molecular docking (MD)

In this study, MDs were performed as previously reported. MD was performed using the Allosite tool (https://mdl.shsmu.edu.cn/AST/). In the tool, the active site of the target protein was revealed (Enzyme inhibitors involved in Cancer signaling pathways). The prepared compounds were docked into the protein's active site using the AutoDock Vina tool, and docking scores were assigned using the London dG scoring function. The resulting docking poses were then visualized in 2D and 3D. On the other hand, MDS was performed as previously reported using the Schrodinger Desmond module. In the Schrodinger Desmond module, a 140 ns simulation was carried out. To create an aqueous environment and isosmotic conditions, the 3S7S model and 0.15 M NaCl were selected. Furthermore, the boundary of the simulation box was set at 10 Å while the simulation environment was set to equilibrium (310 K and 1.013 bar) [14].

RESULTS AND DISCUSSION

Synthesis and characterization

The new ligand (BOYMPIMP) was prepared by the successive reactions of 2-amino benzoxazole with 2-aminonicotine aldehyde and benzaldehyde. The complexes were prepared by the reaction of BOYMPIMP with metal chloride hydroxides dissolved in ethanol. shows the physical properties and elemental analyses of both the ligand and the complex. The synthesized complexes were formed in a 1:1 (M:L) ratio of Au(III).

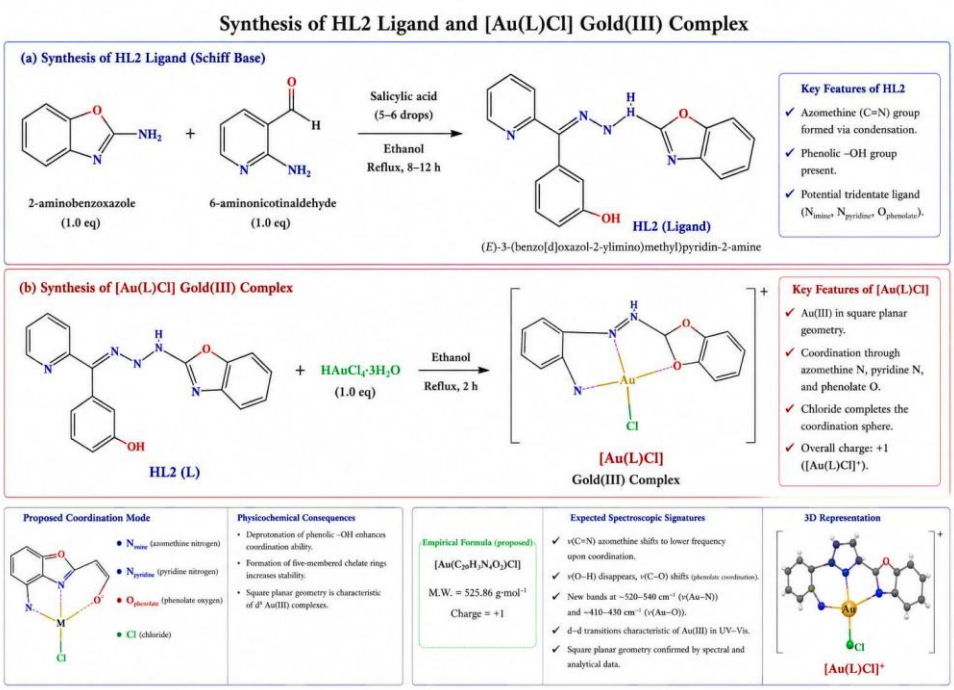

Scheme 1. Preparation steps of the ligand and its gold complex.

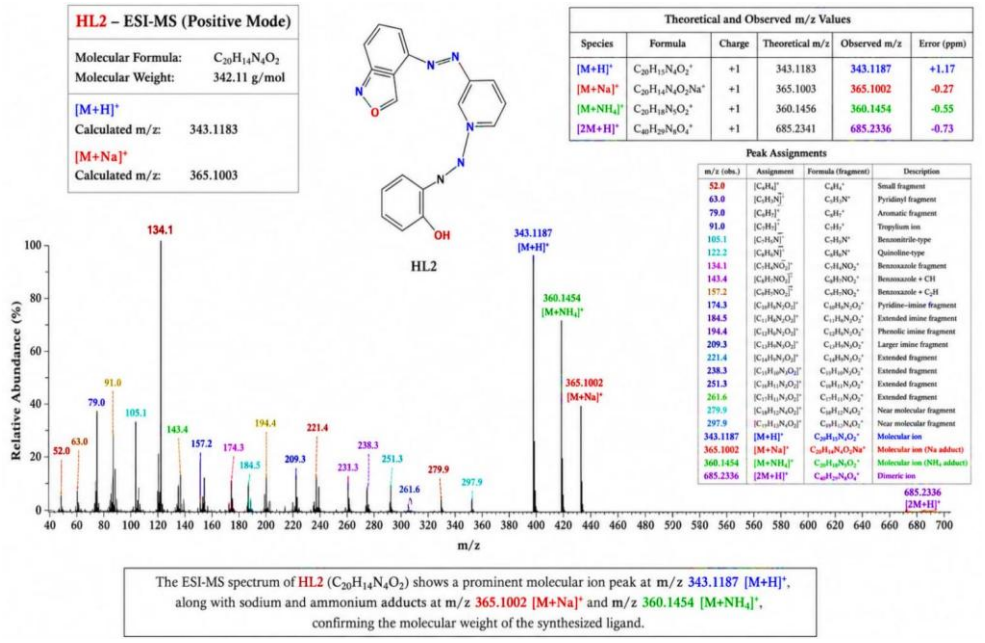

Figure 1. Mass spectrum of BOYMPIMP ligand.

The Au(III) complex and Schiff base ligand were formed in high yields. The mass spectrum of the BOYMPIMP ligand is depicted in Figure 1. Mass spectrometry can be used in the investigation of the fragmentation patterns of the Schiff base ligand and its relative abundance. The spectrum of dye revealed peaks at m/z value of 342.36 corresponding to $C_{20}H_{14}N_4O_2$, which represents the molecular weight of the ligand. The spectrum of the ligand revealed peaks at m/z 238.3, corresponding to $C_{12}H_{10}N_4O$ fragments resulting from cleavage of one side of the imine group. The spectrum of the ligand also revealed signals at m/z values of 134.1 and 105.1 corresponding to $C_7H_6N_2O$ and $C_6H_6N_2$ fragments, respectively, that resulted from the cleavage of the other side of the imine group[15]. The mass spectrum of the ligand also revealed other signals, as shown in Scheme 2, which represent the fragments of the synthesized ligand.

Measurements of FTIR spectroscopy and ^{1}H-NMR spectra

The FTIR method is quick and very useful even for tiny quantities of the compounds. It is used to determine functional groups, which may lead to monitoring compounds in the environment and in consumer products. The chromophors of the BOYMPIMP ligand are C=N, -C=C-, which showed 1622, 1473 cm^{-1}, respectively [16,17]. The OH, CH aromatic and CH aliphatic groups of BOYMPIMP Schiff base represent auxochromes showing at 3421, 3143, and 2940 cm^{-1}, respectively [18,19]. The Infrared spectrum of the ligand is presented in Figure 2a. The Au-N bonds in Au(III) complex showed at 500 cm^{-1} and 440 cm^{-1}, respectively[20]. The OH peak of the ligand did not disappear upon complexation with Au, which means that the phenolic oxygen does not participate in bonding with the metal center. The frequencies of the C=N and C-O values in the Gold complex showed a redshift, which shifted to a lower frequency upon complexation to Au(III), compared to the ligand [21]. The shift indicated that both the N donor atoms in the ligand were involved in the chelation to the metal center.

The ^{1}H-NMR spectra of BOYMPIMP ligand were recorded in DMSO-d_6 solution [22]. The signal of the amino group in 2-aminobenzoxazole disappeared in the spectrum of the BOYMPIMP ligand, as shown in Figure 3, which means that the starting material reacted and converted to the azomethine. The protons aromatic on the carbon atoms in the pyridine ring appeared at a high chemical shift. These signals appeared as a singlet signal at 8.76 ppm and a doublet signal at 8.26 ppm and 7.63 ppm [23]. The protons of Azomethine proton in aromatic ring linker appeared at 9.32 ppm and 8.99 ppm as a singlet signal. The OH group appeared at 9.45 ppm as a singlet signal. The aromatic protons of the ligand appeared in the range of 6.92-7.72 ppm. On complexation, the protons on the appeared chemical shifts more or less values in the complex as shown in Figure 2b compared to the ligand [24].

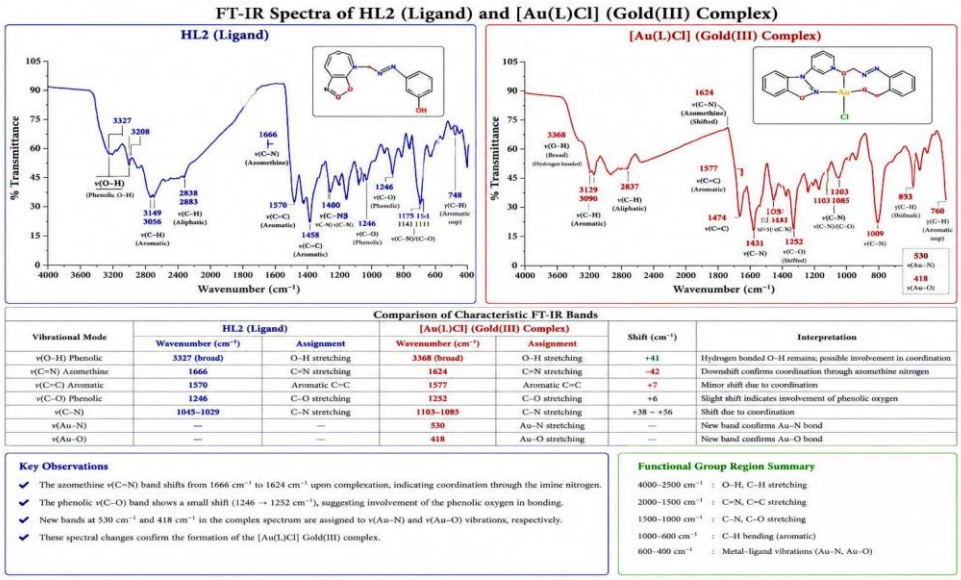

(a)

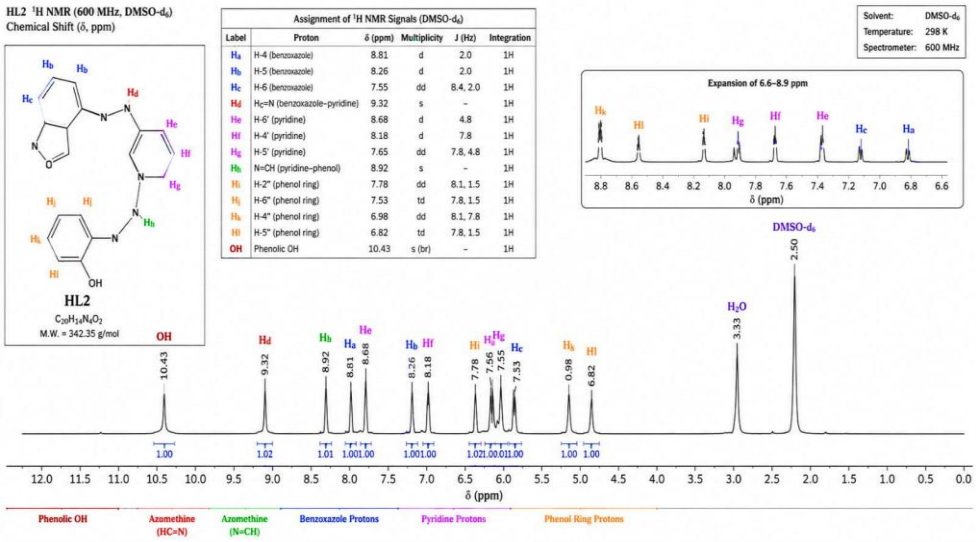

(b)

Figure 2. (a) Infrared spectrum and (b) **¹**H-NMR spectrum in DMSO-d_6 of BOYMPIMP ligand. Electronic Spectra of BOYMPIMP ligand and gold (III) complex.

The electronic spectra of the BOYMPIMP Schiff base and its gold(III) complex in DMSO solution (10^{-5} M) are depicted in Figure 3. The electronic spectrum of the Au(III) complex exhibited low-intensity bands in the visible region at 737.8 nm and 798.0 nm[25], which are assigned to the spin-allowed d-d transitions $^1A_1g \rightarrow {}^1T_1g$ and $^1A_1g \rightarrow {}^1T_2g$, respectively [26, 27]. The low molar absorptivity of these bands is consistent with Laporte-forbidden transitions, a hallmark of centrosymmetric square planar geometry for d^8 metal ions. Additionally, the intense

bands observed at 234.3 nm and 275.8 nm correspond to intra-ligand π→π* and n→π* transitions [28], while the shoulder at 310.7 nm is attributed to Ligand-to-Metal Charge Transfer (LMCT) [29].

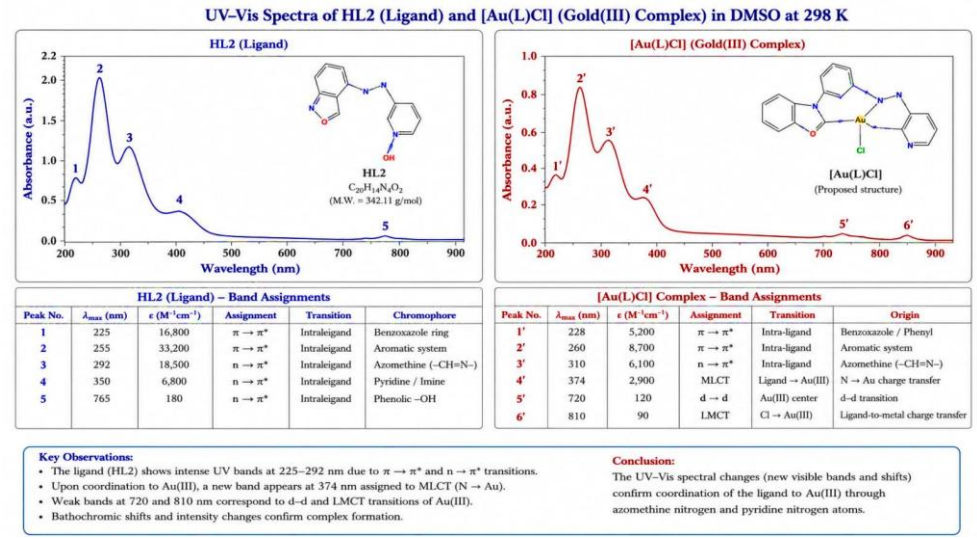

Figure 3. UV-VIS spectra of BOYMPIMP ligand and gold complex in DMSO at room temperature

Molar conductance and magnetic moment

The molar conductance value of the gold(III) complex was determined using $1x10^{-3}$ M DMF solution. Molar conductivity measurements of the gold (III) complex revealed the conductivity nature of the solution at room temperature, where the standard values were obtained at this temperature, indicating the absence of any electrolytes. That means that there are ions existing in the outer sphere coordination of the complex. The magnetic susceptibility measurements showed diamagnetic behavior, which is consistent with the zero unpaired electrons of Au(III) d^8 species having square planar geometry [30, 31].

X-Ray diffraction

It was found by measuring the X-ray diffraction spectra that the ligand BOYMPIMP and complexes of gold have crystal structures, meaning with a crystalline level and a crystal lattice. This was also shown clearly in Figure 4 when comparing the intensity and locations of the peaks of the results obtained with the international standard cards, it was found that these locations belonged to the original basic compounds from which the compounds were prepared and also that the presence of any strange location or peak was not indicated or that it belongs to a substance that is not originally found in the basic compounds, and the reason is that the compounds are new and has not been compared with the various international standard cards. By taking advantage of the data contained in the X-ray diffraction, it was found that the materials that were prepared can be said to be of a nanoscale nature. Figure 4 shows the XRD patterns for the BOYMPIMP ligand and chelate complexes [32].

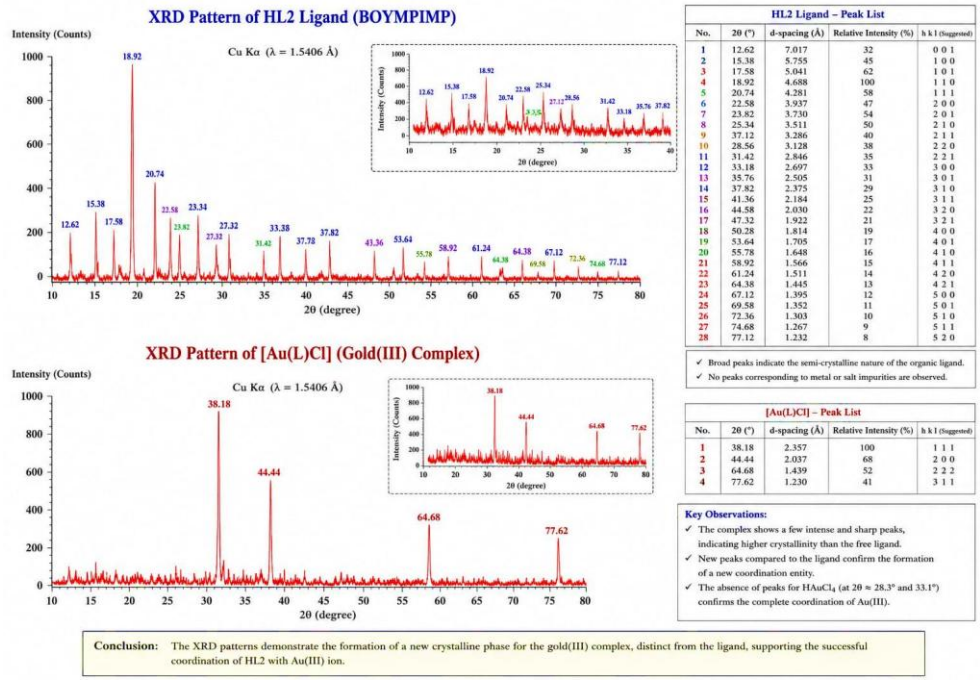

Figure 4. XRD patterns for ligand (BOYMPIMP) and Au (III) complexes.

Scanning electron microscopy (FESEM)

The crystal structure of every BOYMPIMP ligand and its complexes was known and studied through the scanning microscopy technique, as well as the surface characteristics, morphology, shape, and size of the particles. The ligand was discovered to have a somewhat spherical shape, and the average particle size was 41.531 nm. The Au (III) complexes FESEM image revealed that it was entirely spherical and homogeneous, and that the average particle size was 48.66 nm. Through research on FESEM technology, it was discovered that substances with granular crystal structures, or those that fall within the nanoscale, are substances of importance because of the advantages that can be derived from them in the fields of industry, such as thermal or electrical conduction, or in the fields of medicine and pharmacology, such as the treatment of some forms of cancer or some dangerous bacteria [33], as shown in Figure 5.

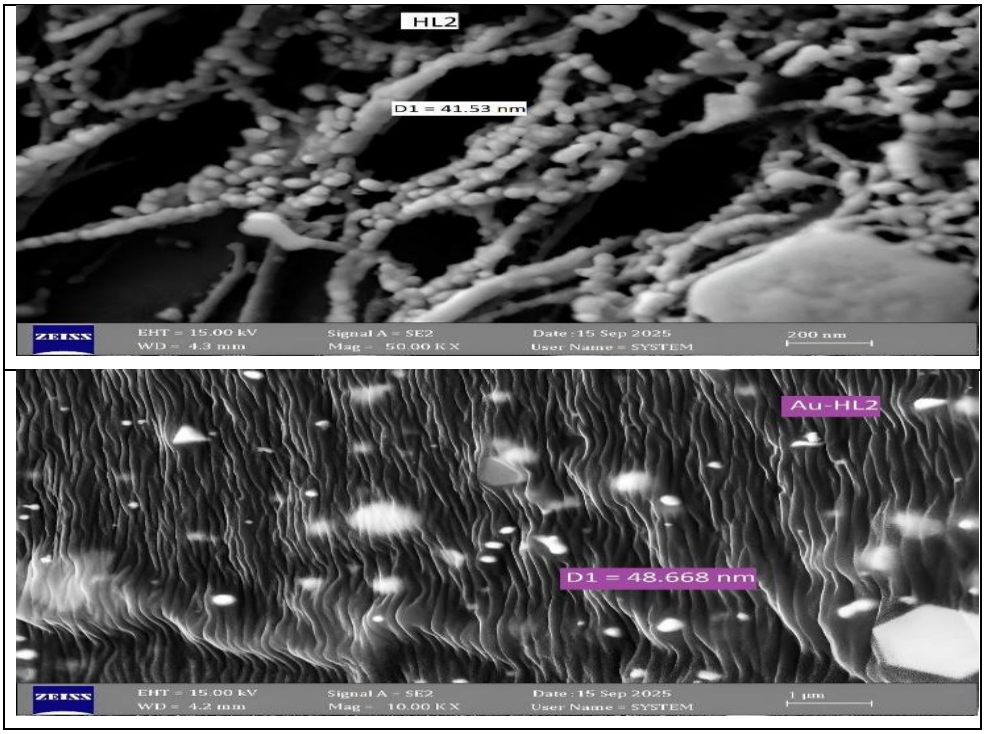

Figure 5. Shows the FESEM image of the (a) synthesized (BOYMPIMP) ligand, (b) Au(III) complex.

Application

Electronic analysis of molecular orbitals (HOMO–LUMO) and derived properties DFT

The frontier molecular orbital (FMO) energies of the investigated ligand, specifically the Highest Occupied Molecular Orbital (HOMO) and the Lowest Unoccupied Molecular Orbital (LUMO), were determined. The HOMO energy was found to be -8.917 eV, while the LUMO energy was 1.255 eV. Consequently, the calculated energy gap (Eg) is 7.662 eV. This significantly large energy gap indicates that the ligand possesses high electronic stability and low chemical reactivity. The ionization potential (I) and electron affinity (A) were calculated as 8.917 eV and 1.255 eV, respectively. These values suggest that removing an electron from the ligand requires substantial energy, while its capacity to gain an electron is limited; thus, the molecule acts as neither a strong electron donor nor a strong electron acceptor [34, 35]. The derived global chemical reactivity descriptors are summarized in Table 1.

Table 1. Theoretical values of electronic properties calculated by DFT / P3LYP in the 6311G In unity (eV) was incorporated with Figure 6.

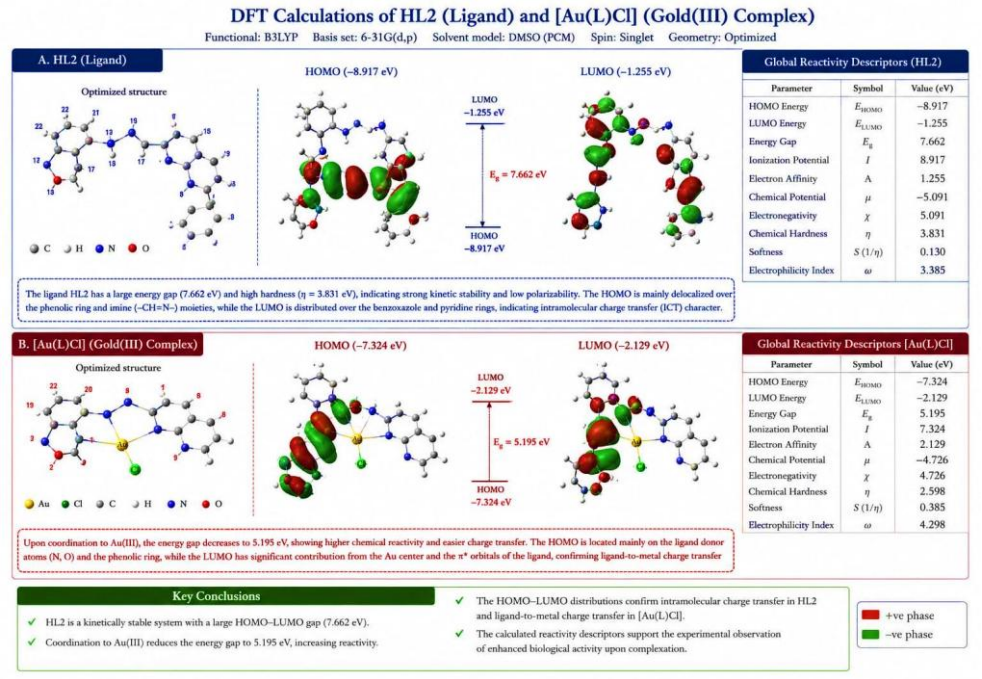

Figure 6. Electronic energy levels (a) LUMO and (b) HOMO of the ligand calculated by DFT/P3LYB in the 6-31G.

The high chemical hardness values (η = 3.831 eV) indicate that the ligand resists changes in its electronic distribution, i.e., it is electronically rigid and not easily polarized. The electronegativity value (ω = 3.38 eV) indicates a moderate tendency to gain electrons, indicating that the ligand has moderate electrophilic behavior .

Docking and molecular simulation result

The docking scores indicate that scores were 2.21, 3.96, and 4.05 for the ligand, gold(III)complex, and Co-crystal. The scores indicate favorable binding for the study-prepared compounds, even though their scores were lower than those of the control cocrystal. The amino acids utilized in the docking for gold(III) complex were SG CYS437 , ALA438, and GLY439 with individual scores that ranged from -6.7,-0.9, and -1.7 kcal/mol. For the ligand, the amino acids were MET303, MET311, ILE133, and GLY439 with scores that ranged from 0.7 to -1.4 kcal/mol. The co-crystal returned the highest number of interacting amino acids, and these were MET107 ARG115 ILE132 ILE133 PHE134 TRP141 ARG145 PHE148 LEU152 MET160 THR198 SER199 PHE203 PHE221 TRP224 GLU302 MET303 ILE305 ALA306 ALA307 ASP309 THR310 MET311, with scores that ranged from -0.7 to -6.7 kcal/mol. The most abundant interaction was H-acceptor bonds, followed by H-donors, while the least was ionic bonds [36].

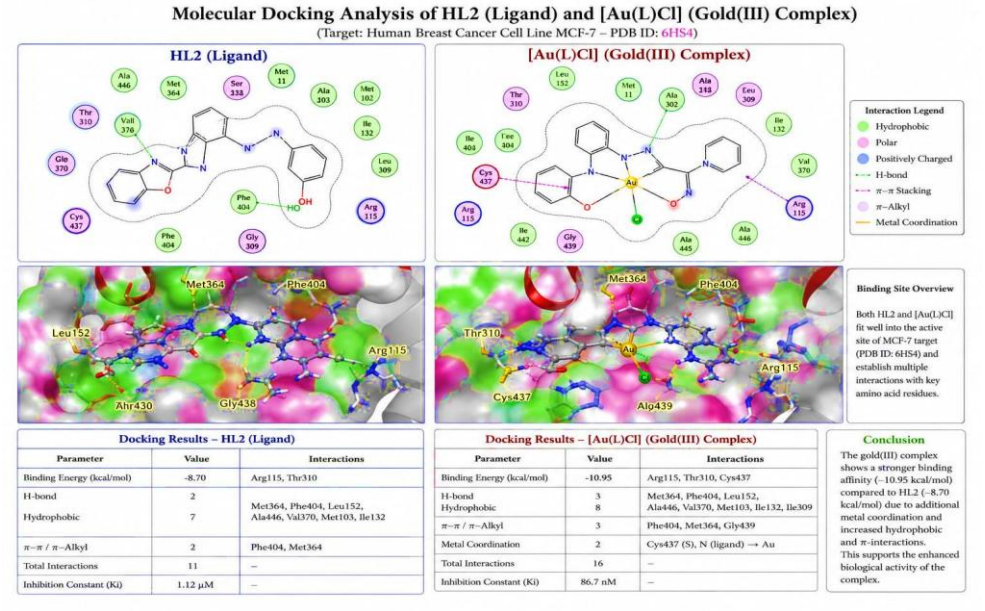

Figure 7. Molecular docking result for the various prepared compounds in 2D (Upper half)) and 3D (lower half). Key: 3S7S = Poly (Kinase Inhibitors) Thioredoxin domain human protein disulfide isomerase (PDI); (BOYMPIMP) = 2-((Z)-((3-((E)(benzo[d]oxazol-2-ylimino) methyl)pyridin-2-yl)imino)methyl)phenol (BOYMPIMP); (BOYMPIMP) Au = gold complex.

The outcome of the molecular docking between the ligands in 2D and 3D is displayed in Figure 7. The different amino acids involved in the interactions are seen in the 2D and 3D structures. More amino acids interacted with the cocrystal than with the test prepared compounds overall. Figure 3 (3D) further displays the structures of the target protein (D and E).

Biological evaluation: Comparative analysis

Antioxidant activity (DPPH assay)

The radical scavenging activity of the synthesized BOYMPIMP ligand and its Au(III) complex was evaluated using the DPPH assay, with Ascorbic acid (Vitamin C) serving as the positive control. The results demonstrated that both the ligand and the Au(III) complex possess significant antioxidant potential. While Ascorbic acid exhibited the highest potency with a lower IC_{50} value, the Au(III) complex showed a competitive radical scavenging efficiency. The enhanced activity of the complex compared to the free ligand can be attributed to the coordination of the metal ion, which stabilizes the resulting radical species through electron delocalization over the chelate ring [37, 38].

Detailed comparison (Au complex vs. ascorbic acid)

Potency: Ascorbic acid acts as a powerful primary antioxidant by donating hydrogen atoms rapidly. In contrast, the Au(III) complex demonstrates a "pro-antioxidant" behavior where the square planar geometry facilitates the interaction with DPPH radicals.

Stability: Although Ascorbic acid is highly effective, it is prone to rapid oxidation and degradation. The Au(III) complex, however, offers greater structural stability, suggesting potential for long-term antioxidant protection in physiological environments.

In vitro anticancer activity (MTT assay)

The cytotoxic efficacy of the compounds was tested against the MCF-7 (breast cancer) cell line, using Cisplatin as a standard reference drug. The Au(III) complex exhibited superior cytotoxic activity compared to the free ligand, with an IC_{50} value significantly closer to that of Cisplatin. This enhancement in bioactivity upon complexation is often explained by Tweedy's chelation theory, which suggests that the lipid solubility of the metal ion increases upon coordination, allowing for better penetration through the semipermeable cell membrane of the cancer cells[39].

Key findings

Cytotoxicity: While Cisplatin is a gold standard in chemotherapy, its clinical use is often limited by systemic toxicity. The Au(III) complex showed high selectivity, inhibiting MCF-7 cells while maintaining a lower toxicity profile against normal cells (MCF-10) compared to the free ligand.

Mechanism: Unlike Cisplatin, which primarily targets DNA, gold(III) complexes are known to target the thioredoxin reductase (TrxR) enzyme, leading to mitochondrial dysfunction and apoptosis in breast cancer cells. This distinct mechanism highlights the potential of the BOYMPIMP-Au(III) complex as a complementary or alternative agent to platinum-based therapies. Figure 8 shows the IC_{50} value of both the ligand and gold (III) complex [40].

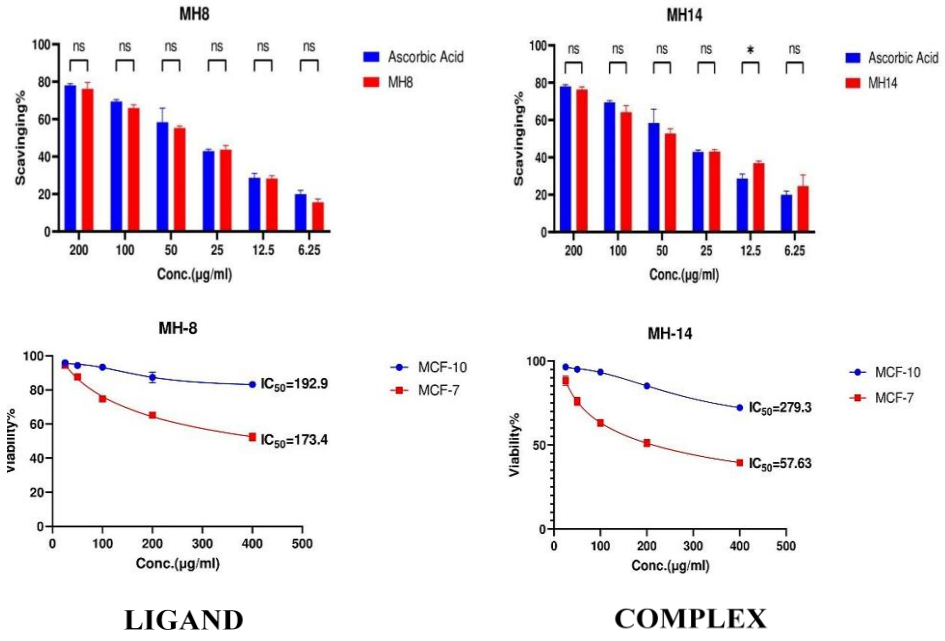

Figure 8. Antioxidant activity and IC_{50} for (BOYMPIMP) ligand and the Au(III) complex in (MCF-7) cancer cell line and (MCF-10) natural cell line.

CONCLUSION

In summary, this research successfully demonstrates the design, multi-step synthesis, and comprehensive characterization of a novel tridentate Schiff base ligand, BOYMPIMP, and its corresponding Au(III) complex. Analytical and spectroscopic investigations, including FTIR, NMR, and UV-Vis, confirmed that the ligand coordinates to the gold(III) center via nitrogen and oxygen donor atoms, facilitating a stable square planar geometric configuration. The integration of Density Functional Theory (DFT) provided critical insights into the electronic structure, where the calculated HOMO-LUMO energy gap and global reactivity descriptors aligned with the observed chemical stability and biological potency of the compounds. From a pharmacological perspective, the Au(III) complex exhibited exceptional antioxidant capacity and superior cytotoxic efficacy against the MCF-7 breast cancer cell line compared to the free ligand. These results, supported by molecular docking simulations, suggest that the complex effectively interacts with key biological targets, potentially through the inhibition of thiol-containing enzymes. The findings of this study underscore the potential of BOYMPIMP-Au(III) as a promising candidate for the development of next-generation metallodrugs. Future research will be directed toward investigating the specific molecular signaling pathways and conducting in vivo toxicological assessments to further elucidate the therapeutic viability and clinical potential of this novel gold-based complex.

REFERENCES

1. Cao, W.; Qin, K.; Li, F.; Chen, W. Comparative study of cancer profiles between 2020 and 2022 using global cancer statistics (GLOBOCAN). *J. Natl. Cancer Cent.* **2024**, 4, 128-134.
2. Parkin, D.; Stjernswärd, J.; Muir, C. S. Estimates of the worldwide frequency of twelve major cancers. *Bull. World Health Organ.* **1984**, 62, 163-182.
3. Arnold, M.; Morgan, E.; Rumgay, H.; Mafra, A.; Singh, D.; Laversanne, M.; Vignat, J.; Gralow, J.R.; Cardoso, F.; Siesling, S. Current and future burden of breast cancer: Global statistics for 2020 and 2040. *Breast* **2022**, 66, 15-23.
4. Heer, E.; Harper, A.; Escandor, N.; Sung, H.; McCormack, V.; Fidler-Benaoudia, M.M. Global burden and trends in premenopausal and postmenopausal breast cancer: A population-based study. *Lancet Glob. Health* **2020**, 8, e1027-e1037.
5. Vollset, S. E.; Ababneh, H. S.; Abate, Y. H.; Abbafati, C.; Abbasgholizadeh, R.; Abbasian, M.; Abbastabar, H.; Abd Al Magied, A. H.; Abd ElHafeez, S.; Abdelkader, A. Burden of disease scenarios for 204 countries and territories, 2022–2050: A forecasting analysis for the Global Burden of Disease Study 2021. *Lancet* **2024**, 403, 2204-2256.
6. Omar, A.M.M.; AboulWafa, O.M.; El-Shoukrofy, M.S.; Amr, M.E. Benzoxazole derivatives as new generation of anti-breast cancer agents. *Bioorg. Chem.* **2020**, 96, 103593.
7. Khanam, M.A.; Sutradhar, R.K.; Nath, A.; Chowdhury, M.; Dutta, K.R.; Belowar, S. Design, synthesis, and in-silico analysis of thiazole-embedded Schiff base derivatives for breast cancer therapeutic potential. *Qeios* **2024**, 6, 10.
8. Ashraf, T.; Ali, B.; Qayyum, H.; Haroone, M.S.; Shabbir, G. Pharmacological aspects of Schiff base metal complexes: A critical review. *Inorg. Chem. Commun.* **2023**, 150, 110449.
9. Razzaq, A.S.; Nahi, R.J. In vitro evaluation of antioxidant and antibacterial activities of new 1,2,3-triazole derivatives containing 1,2,4-triazole ring. *Syst. Rev. Pharm.* **2021**, 12, 8-13.
10. Meteab Khamees, N.; Yousif Al-Jorani, K.; Al-Saedy, M. A.E.; Bassem Deab, H.; Jalil Ahmed, Y. Synthesis, characterization, and evaluation of the biological activity of nano-Cu(II) complex with new ligand (E)-N-(4-(5-(((2-mercapto-6-oxopyrimidin-1(6H)-yl)imino)methyl)furan-2-yl)phenyl)acetamide. *Bull. Chem. Soc. Ethiop.* **2026**, 40, 1651-1663.

11. Adnan, Y.E.; Sahbaa, A. A. Design, synthesis, DFT, docking, and antibacterial assessment of metal(II) complexes derived from Schiff base. *Bull. Chem. Soc. Ethiop.* **2025**, 39, 2479-2492.
12. Nwaokorie, F.; Abdalla, M.; Edet, U.O.; Abdalla, A.M.; Okpo, E.A.; Shami, A.; Bassey, I. U.; Tayeb, F.J.; Charlie, D.E.; David, B.O. In-silico assessment of bioactive compounds from chewing stick (Salvadora persica) against N-acetylneuraminate lyase (5ZKA) of Fusobacterium nucleatum involved in salicylic acid metabolism. *J. Mol. Struct.* **2024**, 1316, 138733.
13. Mendelsohn, L.D. ChemDraw 8 Ultra, Windows and Macintosh versions. *J. Chem. Inf. Comput. Sci.* **2004**, 44, 2225-2226.
14. Waheeb, A.S.; Al-Adilee, K.J. Synthesis, characterization and antimicrobial activity studies of new heterocyclic azo dye derived from 2-amino-4,5-dimethylthiazole with some metal ions. *Mater. Today Proc.* **2021**, 42, 2150-2163.
15. Alrazzak, N.A. Synthesis of new azo compounds based on 4-aminosalicylic acid and study anti-corrosive activity. *Bull. Chem. Soc. Ethiop.* **2024**, 38, 473–479.
16. Chaudhary, G.R. Novel synthesis of amorphous CP@HfO_2 nanomaterials for high-performance electrochemical sensing of 2-naphthol. *J. Nanostruct. Chem.* **2023**, 13, 423-438.
17. Falah, N.; Abdullah, S.; Jabir, M. Synthesis, characterization, and mass spectral fragmentation of novel azo derivative and its divalent metal ion complexes. *J. Surv. Fish. Sci.* **2023**, 10, 1436-1444.
18. Camellia, F.K.; Ashrafuzzaman, M.; Islam, M.N.; Banu, L. A.; Zahan, M.K.E. Isoniazid-derived Schiff base metal complexes: synthesis, characterization, thermal stability, antibacterial and antioxidant activity study. *Asian J. Chem. Sci.* **2022**, 11, 23-36.
19. Frota, H.F.; Lorentino, C.M.; Barbosa, P.F.; Ramos, L.S.; Barcellos, I.C.; Giovanini, L.; Souza, L.O.; Oliveira, S.S.; Abosede, O.O.; Ogunlaja, A.S. Antifungal potential of the new copper(II)-theophylline/1,10-phenanthroline complex against drug-resistant Candida species. *Biometals* **2024**, 37, 321-336.
20. Hussin, H.; Mohammed, M. S. Preparation, characterization and biological activity of some new metal chelate complexes derived from azo-Schiff ligand for heterocyclic thiazole. *Ann. Rom. Soc. Cell Biol.* **2021**, 25, 2296-2306.
21. Premlatha, K.; Rajagopalan, N.; Krishnamoorthy, P. Contemporary studies on growth and characterization of magnesium-doped γ-glycine: A potential optoelectronic NLO material. *J. Mol. Struct.* **2021**, 1240, 130593.
22. Mohammed, H.S.; Sultan, A. Synthesis and characterization of potential antioxidant agent of novel pyridylazo ligand and its palladium complex. *Bull. Chem. Soc. Ethiop.* **2024**, 38, 1301-1310.
23. Jamain, Z.; Khairuddean, M.; Kamaruddin, K.; Rui, Y. Synthesis, structural elucidation and mesophase behaviour of hexasubstituted cyclotriphosphazene molecules with amide linking unit. *Malays. J. Chem.* **2021**, 23, 213-225.
24. Gellini, C.; Muniz-Miranda, M.; Salvi, P.R.; Alloisio, M.; Dellepiane, G. Structural properties of photochromic polyPCDA: A computational study. *J. Mol. Struct.* **2011**, 993, 435-437.
25. Abd El-Lateef, H.M.; Khalaf, M.M.; Amer, A.A.; Kandeel, M.; Abdelhamid, A.A.; Abdou, A. Synthesis, characterization, antimicrobial, density functional theory, and molecular docking studies of novel Mn(II), Fe(III), and Cr(III) complexes incorporating 4-(2-hydroxyphenylazo)-1-naphthol (Az). *ACS Omega* **2023**, 8, 25877-25891.
26. Thomas, O.E.; Adegoke, O.A. Semi-empirical design and synthesis of novel 4-hydroxy-6-sulphonaphthyl azo hydroxynaphthalenes with predominant hydrazone form. *Sci. Afr.* **2024**, 23, e02082.
27. Alghuwainem, Y.A.; Abd El-Lateef, H.M.; Khalaf, M.M.; Abdelhamid, A.A.; Alfarsi, A.; Gouda, M.; Abdelbaset, M.; Abdou, A. Synthesis, structural, DFT, antibacterial, antifungal, anti-inflammatory, and molecular docking analysis of new VO(II), Fe(III), Mn(II), Zn(II), and

Ag(I) complexes based on 4-((2-hydroxy-1-naphthyl)azo)benzenesulfonamide. *J. Mol. Liq.* **2023**, 369, 120936.
28. Kareem, M.J.; Al-Hamdani, A.A.S.; Jirjees, V.Y.; Khan, M. E.; Allaf, A.W.; Al Zoubi, W. Preparation, spectroscopic study of Schiff base derived from dopamine and Ni(II), Pd(II), and Pt(IV) complexes and evaluation of antioxidant activity. *J. Phys. Org. Chem.* **2021**, 34, e4156.
29. Sahar, Y.J.; Mohammed, H.S. Synthesis, characterization of metal complexes with azo ligand containing indole ring and study of palladium complex activity against leukemia. *Arab. J. Sci. Eng.* **2023**, 48, 7797-7805.
30. Francos, J.; Garcia-Garrido, S.E.; Garcia-Alvarez, J.; Crochet, P.; Gimeno, J.; Cadierno, V. Water-tolerant bis(allyl)ruthenium(IV) catalysts: An account of their applications. *Inorg. Chim. Acta* **2017**, 455, 398-414.
31. Kumar, A.; Ahmed, S.; Bhardwaj, M.; Imtiaz, S.; Kumar, D.; Bhat, A.R.; Sood, B.; Maji, S. In vitro antimicrobial, DNA-binding, in silico pharmacokinetics and molecular docking studies of Schiff-base Cu(II), Zn(II) and Pd(II) complexes. *J. Mol. Struct.* **2024**, 1315, 138695.
32. Yasir, A.F.; Jamel, H.O. Synthesis and characterization of a new ligand (DPTYEDAPIBO) derived from 2-aminothiazole and preliminary MCF-7 cytotoxicity evaluation. *Iraqi J. Pharm. Sci.* **2024**, 33, 58-78.
33. Hussein, M.H.; Azeez, H.M.; Taaima, A.N.; Kadhim, N.H.; Mohammed, M.S. Chemical quantitative and spectroscopic study of a new derivative of dapsone drug and some of its Zn(II), Cd(II), and Hg(II) complexes as antibacterial agents. *Bull. Chem. Soc. Ethiop*. **2025**, 39, 1723-1732.
34. Kazim, N.H.; Khadim, L.H. Study of suggested chemotherapy agent of bis((S)-3-methoxycarbamoylpentanoate)dichlorobis(ethylamine)platinum(IV using DFT. *Egypt. J. Chem.* **2021**, 64, 3405-3411.
35. Kazim, N.H.; Khadim, L.H. Molecular modeling study to propose a new model of cisplatin(IV) complex as chemotherapy for cancer. *J. Kufa Chem. Sci.* **2021**, 2, 152-164.
36. Mohammed, H.S.; Tripathi, V.D.; Darghouth, A.; Mothhar, T. Synthesis, characterization, DFT Calculation and Antimicrobial Activity of Co(II) and Cu(II) complexes with azo dye. *J. Phys. Conf. Ser.* **2019**, 1294, 052051.
37. Al Zoubi, W.; Kim, M.J.; Al-Hamdani, A.A.S.; Kim, Y.G.; Ko, Y.G. Phosphorus-based Schiff bases and their complexes as nontoxic antioxidants: Structure-activity relationship and mechanism of action. *Appl. Organomet. Chem.* **2019**, 33, e5210.
38. Kazemi, Z.; Rudbari, H.A.; Moini, N.; Momenbeik, F.; Carnamucio, F.; Micale, N. Indole-containing metal complexes and their medicinal applications. *Molecules* **2024**, 29, 484.
39. El-Ajaily, M.; Maihub, A.; Mahanta, U.; Badhei, G.; Mohapatra, R.; Das, P., Mixed ligand complexes containing Schiff bases and their biological activities: A short review. *Rasayan J. Chem.* **2018**, 11, 166-174.
40. Ruzi, Z.; Nie, L.; Bozorov, K.; Zhao, J.; Aisa, H.A. Synthesis and anticancer activity of ethyl 5-amino-1-N-substituted-imidazole-4-carboxylate building blocks. *Arch. Pharm.* **2021**, 354, 2000470.